J. Shanghai Jiao Tong Univ. (Sci.), 2023
https://doi.org/10.1007/s12204-023-2634-7

Load Stability Analysis of a Floating Multi-Robot Coordinated Towing System

SU Cheng (苏　程), *ZHAO Xiangtang* (赵祥堂), *YAN Zengzhen* (闫增祯), *ZHAO Zhigang** (赵志刚), *MENG Jiadong* (孟佳东)
(School of Mechanical Engineering, Lanzhou Jiaotong University, Lanzhou 730070, China)

Abstract: Cranes used at sea have some shortcomings in terms of flexibility, efficiency, and safety. Therefore, a floating multi-robot coordinated towing system is planned to fulfill the offshore towing requirements. It is difficult to study the stability of a floating multi-robot coordinated towing system by ancient strategies. First, the minimum tension of the rope and the minimum singular value of the stiffness matrix were separately used to analyze the load stability. The advantages and disadvantages of the two methods were discussed. Then, the two stability analysis methods were normalized and weighted to obtain the method based on minimum tension and minimum singular to comprehensively analyze the stability of the load. Finally, the effect of different weighting coefficients on the load stability was analyzed, which led to a reasonable weighting coefficient to evaluate the load stability by comparing with a single analysis method. The research results provide a basis for the motion planning and coordinated control of the towing system.

Key words: offshore towing, multi-robot system, load stability, minimum tension, minimum singular
CLC number: TH 113, TP 242.2　　**Document code:** A

0 Introduction

In recent years, with the rapid rise of the robotics industry, researchers have gradually applied industrial robots to offshore towing, additionally exploiting the benefits of high flexibility and large carrying capacity of robots. In some towing operations, a single robot is commonly unable to fulfill the particular needs; thus a multi-robot coordinated towing system has been developed[1]. At present, the multi-robot coordinated towing system is principally divided into three categories. One is the traditional ground multi-robot towing system[2-3], which may undertake massive load operations; the theory has been comparatively mature. Another is the aerial multi-robot towing system[4-6], the towing cost of this sort of robot is high, but its carrying capacity is restricted, and it can only lift objects with tiny loads. The third type is to place the towing robot on a floating platform for water towing. This system contains a large carrying capacity and high flexibility, but the related research has just been carried out. With the deepening of ocean exploration, the floating multi-robot coordinated towing system has been applied more widely, which can meet the common requirements of current maritime salvage operations[7-9].

The floating multi-robot coordinated towing system belongs to the class of under-constrained systems that are sensitive to external disturbances. When the system is subjected to a large external force, or a heavy load, it may overturn. It is dangerous to use real objects in stability experiments, so it is necessary to carry out theoretical analysis and simulations of the load stability of the towing system, which can be used as a reference for practical applications of towing system.

The stability of a floating multi-robot coordinated towing system can be divided into static and motional stability from the state of motion, load and floating base stability from the structural composition of the towing system, and structural and control stability from the specific form of stability. In recent years, stability in robotics has been studied by several scholars with several achievements. Michael et al.[10] analyzed the structure of the multi-robot towing system, and took whether the Hessian matrix was positive definite as the criterion for the static stability. If the eigenvalues were all positive, the system would be stable, but the effect of the rope tension on the towing

Received: 2022-10-11　**Accepted:** 2023-01-09
Foundation item: the National Natural Science Foundation of China (No. 51965032), the Natural Science Foundation of Gansu Province (No. 22JR5RA319), the Science and Technology Foundation of Gansu Province (No. 21YF5WA060) and the Excellent Doctoral Student Foundation of Gansu Province (No. 23JRRA842)
∗**E-mail:** zhaozhg@mail.lzjtu.cn

system was neglected and the system may be unstable. Bosscher[11] analyzed the stability of the towing system based on the curvature of the trajectory of the load, but ignored the influence of rope tension on the system. Behzadipour and Khajepour[12] took the total stiffness of the under-constrained parallel system as the criterion to analyze the stability of the system, but the system may be unstable when the stiffness matrix is an asymmetric matrix. Carricato and Merlet[13] proposed the under-constrained rope parallel system; the stability was judged by optimizing the binding force. These evaluation methods all use a single evaluation criterion to judge the stability of the system. Since many factors are related to stability, influence factors can be added to the hybrid stability evaluation approach to assess the stability of the system more comprehensively. In Refs. [14-15], the tension distribution of ropes in the workspace of the parallel mechanism was used; the stability of multi-robot towing system was analyzed by the force-position index; this method considered two factors: the position of the load and the distribution of the rope tension. In Refs. [16-17], the stability of a multi-robot coordinated towing system with fixed base was studied; the influence of load posture on stability was further considered. A combined force-position-pose method was proposed to analyze the stability of the towing system. Then, the stiffness factor was added to the hybrid stability evaluation method, but the influence of each factor on the stability under different weighting coefficients is not analyzed[18]. Most of the systems mentioned above are rope-driven parallel systems applied to the ground, where the robot has a fixed base and the rope tension does not affect the movement trajectory of the towing robot. The rope tension of a floating multi-robot coordinated towing system can affect the trajectory of the towing robot, and then force-coupling phenomena can occur in the system. Therefore, as a relatively new research direction, this system is not only of high engineering application value, but also of new interest for related theoretical studies of rope-driven parallel mechanisms.

The floating multi-robot coordinated towing system uses multiple ropes to control the movement of the load in a floating environment. The number of ropes in the system is smaller than the number of degrees of freedom of the load, which is an under-constrained system. The balance of the load is required, depending on its own gravity and inertial forces, and it is weakly resistant to external disturbances. The load stability of the towing system is the focus of this study. The above-mentioned literature has analyzed the stability of rope-driven parallel systems from different perspectives. Most scholars have used rope tension and stiffness for their analysis, but systems in which the number of ropes is greater than or equal to the number of degrees of freedom of the load have mostly been studied from control algorithms. Inspired by the above analysis, we analyzed the stability of the load using the minimum tension of the rope and the minimum singular value of the stiffness matrix, separately. To improve the applicability of the method, we proposed the evaluation method based on minimum tension and minimum singularity. Based on the distribution map and the contour map of stability, the distribution of load stability was discussed under different combinations of the weighting coefficients. According to the simulation results, choosing the optimal weighting coefficient can avoid the load from working in the unstable area, and ensure that the stability does not generate large fluctuations.

1 System Configuration

The floating multi-robot coordinated towing system consists of floating robots and a rope-driven parallel towing system. The structure of the towing system is shown in Fig. 1. The following coordinate systems are established according to the structure of the towing system. In the coordinate system O-XYZ, the end position of the floating robot is $\boldsymbol{A}_i = (x_{ai}, y_{ai}, z_{ai})^{\mathrm{T}}$, $\boldsymbol{L}_i$ is the position vector of the rope, and the junction point between the rope and the suspended load is $\boldsymbol{B}_i = (x_{bi}, y_{bi}, z_{bi})^{\mathrm{T}}$. To analyze the dynamics of the floating robot, it is necessary to establish the coordinate systems O_i-$X_iY_iZ_i$ for each floating base, and the origin of each coordinate system is established at the center of the section of the floating base and the horizontal plane. The coordinate system O'-$X'Y'Z'$ is established at the barycenter of the suspended load. The Z' axis is perpendicular to the upper surface of the load. The position $\boldsymbol{r} = (x, y, z)^{\mathrm{T}}$ and the angle $(\alpha, \beta, \gamma)^{\mathrm{T}}$ of the coordinate system O'-$X'Y'Z'$ with respect to the coordinate system O-XYZ are the position vector and attitude angle of the suspended load. The rod length of the robot is (a_{i1}, a_{i2}, a_{i3}), and the joint angle is $(\varphi_{i1}, \varphi_{i2}, \varphi_{i3})$. Since the whole system consists of three towing robots,

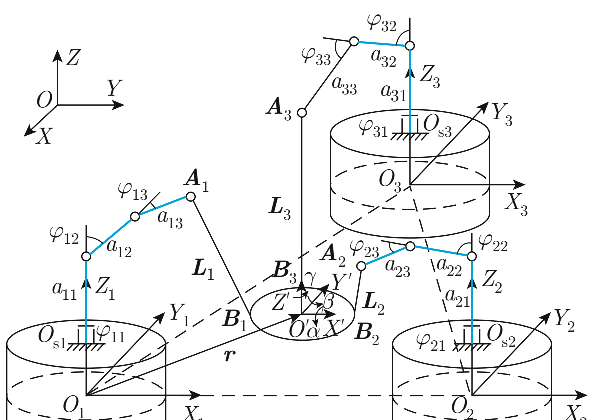

Fig. 1 Structure of floating multi-robot coordinated towing system

thus $i = 1, 2, 3$. The load is moved in the desired trajectory by adjusting the robot end position or the length of the rope. The rope is adjusted by the actuator at the robot end.

According to the structure of the towing system, the complete towing process is divided into three stages. To reduce interference from external factors, a driving mode is chosen for different towing stages.

(1) In the first stage, the load needs to be lifted in the vertical direction; the driving mode of the towing system is to fix the end position of the robot and adjust the length of the rope.

(2) In the second stage, the position of the load in space changes greatly; the driving mode of the towing system is to keep the length of the rope unchanged and adjust the end position of the robot.

(3) In the third stage, since the position and posture of the load need to be changed, but the amount of change is small, the towing system's driving mode is that the rope length and the end position of the robot change at the same time.

2 Dynamic Analysis

Due to the complex structure of the actual towing system, the following assumptions were made in the stability analysis without affecting the analytical results:

(1) The barycenter of the three floating robots is distributed in a regular triangle on the horizontal plane, the floating robot is a rigid body with uniform mass, and the elastic deformation will not occur under the action of external force.

(2) The influence of the change of the center of gravity of the whole system on the position and posture of the floating base is ignored during towing.

(3) The rope is regarded as an ideal rigid body, its mass and elastic deformation are ignored, and the rope can swing freely at the end of the robot.

(4) Constrained by the balancing device, the floating base only has a heave motion along the vertical direction, and the heave motion of the base does not change the state of the water surface.

2.1 Dynamic Analysis of a Rope-Driven Parallel Towing System

Herein, $\boldsymbol{B}_i'$ is the position of the junction point between the rope and the load in O'-$X'Y'Z'$ and $\boldsymbol{B}_i'$ is a 3×1 vector. The positions of the ropes are represented as follows:

$$\boldsymbol{L}_i = \boldsymbol{A}_i - \boldsymbol{B}_i, \tag{1}$$

$$\boldsymbol{B}_i = \boldsymbol{R}\boldsymbol{B}_i' + \boldsymbol{r}. \tag{2}$$

In Eq. (2), $\boldsymbol{R}$ is the transformation matrix of the O'-$X'Y'Z'$ relative to the O-XYZ with size of 3×3:

$$\begin{aligned}\boldsymbol{R} =& \operatorname{Rot}(z,\gamma)\operatorname{Rot}(y,\beta)\operatorname{Rot}(x,\alpha) = \\ & \begin{bmatrix} \cos\gamma & -\sin\gamma & 0 \\ \sin\gamma & \cos\gamma & 0 \\ 0 & 0 & 1 \end{bmatrix} \begin{bmatrix} \cos\beta & 0 & \sin\beta \\ 0 & 1 & 0 \\ -\sin\beta & 0 & \cos\beta \end{bmatrix} \begin{bmatrix} 1 & 0 & 0 \\ 0 & \cos\alpha & -\sin\alpha \\ 0 & \sin\alpha & \cos\alpha \end{bmatrix} = \\ & \begin{bmatrix} \cos\beta\cos\gamma & \cos\gamma\sin\beta\sin\alpha - \cos\alpha\sin\gamma & \sin\gamma\sin\alpha + \cos\gamma\cos\alpha\sin\beta \\ \cos\beta\sin\gamma & \cos\alpha\cos\gamma + \sin\gamma\sin\beta\sin\alpha & \sin\gamma\sin\beta\cos\alpha - \cos\gamma\sin\alpha \\ -\sin\beta & \cos\beta\sin\alpha & \cos\alpha\cos\beta \end{bmatrix}.\end{aligned} \tag{3}$$

The balance equation of the load is established by using the force spinor balance principle as follows:

$$\boldsymbol{J}^{\mathrm{T}}\boldsymbol{T} = \boldsymbol{F}_{\mathrm{o}}, \tag{4}$$

where, $\boldsymbol{T} = [T_1 \;\; T_2 \;\; T_3]^{\mathrm{T}}$, $T_{\min}^{\mathrm{s}} \leqslant T_i \leqslant T_{\max}^{\mathrm{s}}$; $T_{\min}^{\mathrm{s}}$ and $T_{\max}^{\mathrm{s}}$ are the minimum pre-load tension and maximum allowable tension of the rope, respectively. In Eq. (4), $\boldsymbol{F}_{\mathrm{o}}$ is the external force and torque acting on the load with size of 6×1:

$$\boldsymbol{F}_{\mathrm{o}} = \left(\left(M_{\mathrm{f}}\frac{\mathrm{d}\boldsymbol{v}}{\mathrm{d}t}\right)^{\mathrm{T}}, \left((J_x, J_y, J_z)\frac{\mathrm{d}\boldsymbol{\omega}}{\mathrm{d}t}\right)^{\mathrm{T}}\right)^{\mathrm{T}}, \tag{5}$$

where, M_{f} is the mass of the load; J_x, J_y, J_z are the inertia torque of the load; $\boldsymbol{v} = \dot{\boldsymbol{r}} = (\dot{x}, \dot{y}, \dot{z})^{\mathrm{T}}$ and $\boldsymbol{\omega} = (\dot{\alpha}, \dot{\beta}, \dot{\gamma})^{\mathrm{T}}$ are the linear and angular velocity of the load, respectively.

Additionally, $\boldsymbol{J}^{\mathrm{T}} = [\boldsymbol{J}_1 \;\; \boldsymbol{J}_2 \;\; \boldsymbol{J}_3]$ is the structure matrix of the towing system with size of 6×3:

$$\boldsymbol{J}_i = \begin{bmatrix} \boldsymbol{e}_i \\ (\boldsymbol{R}\boldsymbol{B}_i') \times \boldsymbol{e}_i \end{bmatrix}, \quad i = 1, 2, 3, \tag{6}$$

where $\boldsymbol{e}_i = \boldsymbol{L}_i / \|\boldsymbol{L}_i\|$ is the unit vector of the rope length.

2.2 Dynamic Analysis of Floating Robots

Assuming that the three floating robots have the same structure, one of them is selected as an example for dynamic modeling. It is assumed that the floating robot does not roll when it makes a heaving motion under the action of a regular wave. The motion equation of a floating robot subjected to external forces is

$$\boldsymbol{M}\ddot{\boldsymbol{z}} = \boldsymbol{F}, \tag{7}$$

where, $\boldsymbol{z}$ is the vertical displacement of the floating robot with size of 3×1; $\boldsymbol{M}$ is the mass matrix with size of 3×3; $\boldsymbol{F}$ is the external force, including buoyancy, fluid restoring force, damping force, wave disturbance force and the rope tension, acting on the floating robot with size of 3×1. The dynamic equation of the floating robot is

$$\boldsymbol{M}\ddot{\boldsymbol{z}} + \boldsymbol{C}\dot{\boldsymbol{z}} + \boldsymbol{K}\boldsymbol{z} = \boldsymbol{F}_{\mathrm{e}}, \tag{8}$$

where $\boldsymbol{M}$ consists of an additional mass matrix $\boldsymbol{M}_{\mathrm{a}}$ and a structural mass matrix $\boldsymbol{M}_{\mathrm{s}}$. According to Ref. [7], the mass matrix can be obtained as follows:

$$\boldsymbol{M} = (\boldsymbol{M}_{\mathrm{a}} + \boldsymbol{M}_{\mathrm{s}}) = \begin{bmatrix} m_{11} + m_{\mathrm{G}} & 0 & 0 \\ 0 & m_{22} & 0 \\ 0 & 0 & m_{33} \end{bmatrix}, \tag{9}$$

where $m_{11} = 4\rho r^3/3$, ρ is the density of water, r is the radius of the floating base, and m_{G} is the mass of the floating robot. Similarly, the expressions for m_{22} and m_{33} can be obtained.

In Eq. (8), $\boldsymbol{C}$ is the nonlinear viscous damping coefficient matrix without considering the coupling of each degree-of-freedom, whose size is 3×3, and the viscous damping of heave motion can be calculated by using the empirical formula with reference to the Froude-Krylov hypothesis[9].

In Eq. (8), $\boldsymbol{K}$ is the stiffness matrix with size of 3×3, and only the static stiffness of the floating robot is analyzed, then:

$$\boldsymbol{K} = \begin{bmatrix} \rho g \pi r^2 & 0 & 0 \\ 0 & 2\rho g \pi r^3(l_1 - l_2) & 0 \\ 0 & 0 & 2\rho g \pi r^3(l_1 - l_2) \end{bmatrix}, \tag{10}$$

where g is the acceleration of gravity, l_1 is the distance from the center of the floating robot to the water surface, and l_2 is the distance from the center of the buoyancy of the floating robot to the water surface.

Additionally, $\boldsymbol{F}_{\mathrm{e}}$ is the external force acting on the floating robot whose size is 3×1. The external force on the floating base is the rope tension, which can be obtained according to Eq. (4).

3 Stability Analysis

The ability of a load to recover its initial position and pose after external interference is called the stability of the load. The floating multi-robot coordinated towing system is an under-constrained system, and the balance of the load must rely on gravity and inertial forces to be maintained. Due to the flexibility of the rope-driven parallel robot, the unidirectional pulling property of the rope, and the floating characteristic of the base, it is easy to overturn the towing system. Therefore, the qualitative analysis of whether the load is stable or not does not fit the actual requirements, and the stability of the load in the workspace must be analyzed in conjunction with the actual situation.

3.1 Stability Analysis Based on Minimum Tension of Rope

The rope tension of the towing system is divided into a vertical component which resists the gravity of the load, and a horizontal component that resists the tension of the other two ropes. The force of the rope is positively correlated with the degree of tension of the rope. The tighter the rope, the greater the external force required to counteract the load, indicating a higher stability of the load. Therefore, the minimum tension of the rope can be used to analyze the stability of the load, and the larger the minimum tension, the more stable the load of the towing system.

The load is pulled by three ropes in the towing system, and the stability of the load can be judged by the minimum tension of the ropes using a short-plate effect analysis. Given the trajectory of the load, the tension curves of the corresponding three ropes can be obtained. The minimum tension of the three ropes can be expressed as follows:

$$T_{\min} = \min(\boldsymbol{T}) = \min(T_1, T_2, T_3). \tag{11}$$

The distribution of the three floating robots is an equilateral triangle, and due to the symmetry of the structure, the pulling force of the three ropes on the vertical line of the workspace is equal to the minimum tension $T_{\min}$:

$$T_i = T_{\min} = \frac{M_{\mathrm{f}} g}{3\cos\theta}, \tag{12}$$

where θ represents the angle between the rope and the vertical line of the workspace, and the range of θ can be calculated according to the coordinates of the lowest point and the highest point of the load in the workspace, so the minimum and maximum values of the rope tension of the towing system can be calculated.

Since the direction of the tension is always the same as the direction of the rope, the force that balances the load is the vertical component of the rope. When the load is perturbed by an external force, the tension of the rope changes instantaneously. Results of load stability analysis are given according to minimum tension; the minimum tension of the rope increases, the position of the load shrinks to the upper part of the workspace, but the shrinkage speed is different, indicating that the equivalent points of the minimum tension in the workspace are not evenly distributed. Therefore, there are certain limitations in using the minimum tension of the rope to analyze the load stability of the towing system.

3.2 Stability Analysis Based on Minimum Singularity of Stiffness Matrix

Stiffness is the ability of a material to resist elastic deformation when subjected to external forces. The stiffness of a towing system is the degree to which the position and pose of the load change when the load is subjected to external forces. The stiffness of the load at any position in the workspace can be represented by a matrix. If the stiffness of the position is larger, it is harder to deviate from the original position, indicating that the position is more stable. Therefore, the stiffness can be used to measure the load stability of the towing system.

The rope stiffness is infinite in the inelastic linear model, so the rope model needs to be further standardized for the analysis of the stiffness.

(1) The rope is an ideal rope model, which only bears the tension and produces elastic deformation when subjected to external forces.

(2) The connection point between the rope and the end of the robot, and the connection point between the rope and the load are all ideally articulated; the deformation at the articulated point is zero.

The stiffness $\boldsymbol{K}$ of a towing system is defined as the ratio of the variation of the external force vector to the variation of the position and pose of the load:

$$\boldsymbol{K} = \frac{\mathrm{d}\boldsymbol{F}}{\mathrm{d}\boldsymbol{X}}. \tag{13}$$

Since both the rope tension $\boldsymbol{T}$ and the structure matrix $\boldsymbol{J}$ are functions of $\boldsymbol{X}$ (the position and pose of the load), the stiffness of the towing system is the superposition of the structure change and the tension change:

$$\boldsymbol{K} = \frac{\mathrm{d}\boldsymbol{F}}{\mathrm{d}\boldsymbol{X}} = \frac{\mathrm{d}\boldsymbol{T}}{\mathrm{d}\boldsymbol{X}}\boldsymbol{J} + \frac{\mathrm{d}\boldsymbol{J}}{\mathrm{d}\boldsymbol{X}}\boldsymbol{T} = \boldsymbol{K_T} + \boldsymbol{K_J}, \tag{14}$$

where $\boldsymbol{K_J}$ is the stiffness arising from the change of position and pose of the load when it is subjected to the external forces, and is therefore called structural change stiffness; $\boldsymbol{K_T}$ is the stiffness caused by the change of rope tension, so it is called tension change stiffness[19]. The full expression for the stiffness matrix of the towing system will not be derived here in detail.

The load stability of the towing system is not to determine whether a certain position is stable, but rather to analyze the degree of stability of the load at different positions in the workspace. Therefore, combined with the characteristics of the towing system, the relevant knowledge about eigenvalues and symmetric matrices in matrix theory is used[20], and a scalar index which can characterize the stiffness performance is proposed to analyze the load stability. That is, the stability of the load is analyzed based on the singular value $\sigma(\boldsymbol{K})$ of the stiffness matrix, and the smaller the minimum singular value $\sigma_{\min}(\boldsymbol{K})$ of the stiffness matrix, the weaker the stiffness and the worse the stability of the load at that position.

3.3 Stability Analysis Based on Minimum Tension and Minimum Singularity

While the minimum tension and the minimum singular value of the stiffness matrix can be used to analyze the stability of the load separately, the stability of the load is prone to deviations from a single aspect. Thus, the stability of the load can be analyzed by combining the minimum tension and the minimum singular value of the stiffness matrix. Different factors have different effects on load stability, so it is necessary to make a distinction in magnitude. After data standardization, the minimum tension $T_{\min}$ and the minimum singular value $\sigma_{\min}(\boldsymbol{K})$ of the stiffness matrix are mapped to the interval [0, 1] in proportion, and the two are superimposed by the weighting method. In this way, a comprehensive index for analyzing load stability is obtained:

$$\phi = k_1 \frac{T_{\min}}{T_{\min}^{\max}} + k_2 \frac{\sigma_{\min}(\boldsymbol{K})}{\sigma_{\min}^{\max}(\boldsymbol{K})}, \tag{15}$$

where $T_{\min}^{\max}$ represents the maximum of the minimum tension of the three ropes; $\sigma_{\min}^{\max}(\boldsymbol{K})$ represents the maximum of the minimum singular value of the stiffness matrix; k_1 and k_2 are the weighting coefficients, and $k_1 + k_2 = 1$ is satisfied.

In summary, the stability degree is obtained by weighting the minimum tension of the rope and the minimum singular value of the stiffness matrix, which basically synthesizes the advantages of the two and effectively resolves the drawbacks when they are used separately as evaluation indexes.

4 Simulation Analysis

The three floating robots are arranged in an equilateral triangle in space, and the ends of the three robots are kept at the same height. The projection of the towing system in the initial state is shown in Fig. 2. The initial positions of the barycenters and endpoints of the three floating robots are shown in Table 1. The structure of the floating base is a cylinder with height $h = 1\,\mathrm{m}$ and radius $r = 0.5\,\mathrm{m}$. The parameters of the robot are given in Table 2. The draft depth of the floating robot resting on the water

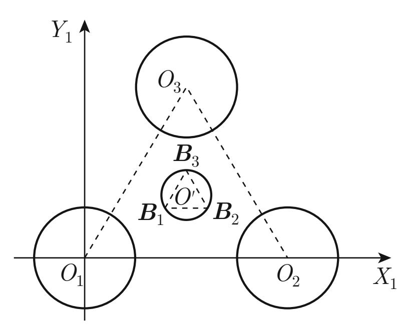

Fig. 2 Projection of the towing system on the $X_1O_1Y_1$ plane

surface is 0.5 m, the draft-weight is 392.4 kg, and the fluid density is $\rho = 10^3\,\mathrm{kg/m^3}$. The mass of the load is 10 kg, the rope length is 0.5 m to 3 m, and the initial position of the load is (1.5, 1.25, 1) m. The radius of the load is 0.1 m, and the junction points between the ropes and the load are $\boldsymbol{B}_1 = (-0.05\sqrt{3}, -0.05, 0)^{\mathrm{T}}$ m, $\boldsymbol{B}_2 = (0.05\sqrt{3}, -0.05, 0)^{\mathrm{T}}$ m, and $B_3 = (0, 0.1, 0)^{\mathrm{T}}$ m.

Table 1 Initial coordinates of the floating robot

Point	X/m	Y/m	Z/m
O_1	0	0	0
O_2	3	0	0
O_3	1.5	$1.5\sqrt{3}$	0
$\boldsymbol{A}_1$	1	$5\sqrt{3}/6$	1.5
$\boldsymbol{A}_2$	1	$-2\sqrt{3}/3$	1.5
$\boldsymbol{A}_3$	7/4	$\sqrt{3}/12$	1.5

Table 2 Parameters of the robot

Parameter	Value
φ_{11}/rad	$\left(-\frac{\pi}{2}, \frac{\pi}{2}\right)$
φ_{21}/rad	$\left(\frac{\pi}{2}, \frac{3\pi}{2}\right)$
φ_{31}/rad	$(-\pi, 0)$
$\varphi_{i2}, \varphi_{i3}$/rad	$\left(\frac{\pi}{12}, \frac{5\pi}{12}\right)$
a_{i1}/m	1
a_{i2}/m	0.5
a_{i3}/m	0.5

The equations of motion for the barycenter of the load at the time t are assumed to be

$$\left.\begin{aligned} x &= 0.5\cos(0.4\pi t) \\ y &= 0.5\sin(0.4\pi t) \\ z &= 0.05t \\ \alpha &= \beta = \gamma = 0 \end{aligned}\right\}. \tag{16}$$

Based on the expected trajectory of the load, combined with the dynamics of the towing system, the parameters can be calculated to obtain $T_{\min}^{\max} = 339.25$ N, $\sigma_{\min}^{\max} = 2.878\,9 \times 10^4$ N/m. In the same towing environment, if the chosen weighting coefficients are different, the resulting stability is also different. How to choose the weighting coefficients is the research difficulty of the method. The stability of the first stage of the towing system is studied. Figures 3—5 show the stability (ϕ) distributions obtained in the plane $Z = 1$ m, $Y = 0.866$ m and $X = 1.5$ m when taking three sets of weighting coefficients, respectively. Different colors represent different stability, which increases continuously from cool to warm colors. It is clear from the figures that the closer the load is to the central point of the triangle in the same horizontal plane, the higher the stability of the load. The closer the load is to the top of the workspace, the higher the stability of the load in the workspace.

It can be clearly seen from Figs. 3—5, with the increase of the weighting coefficient of the minimum

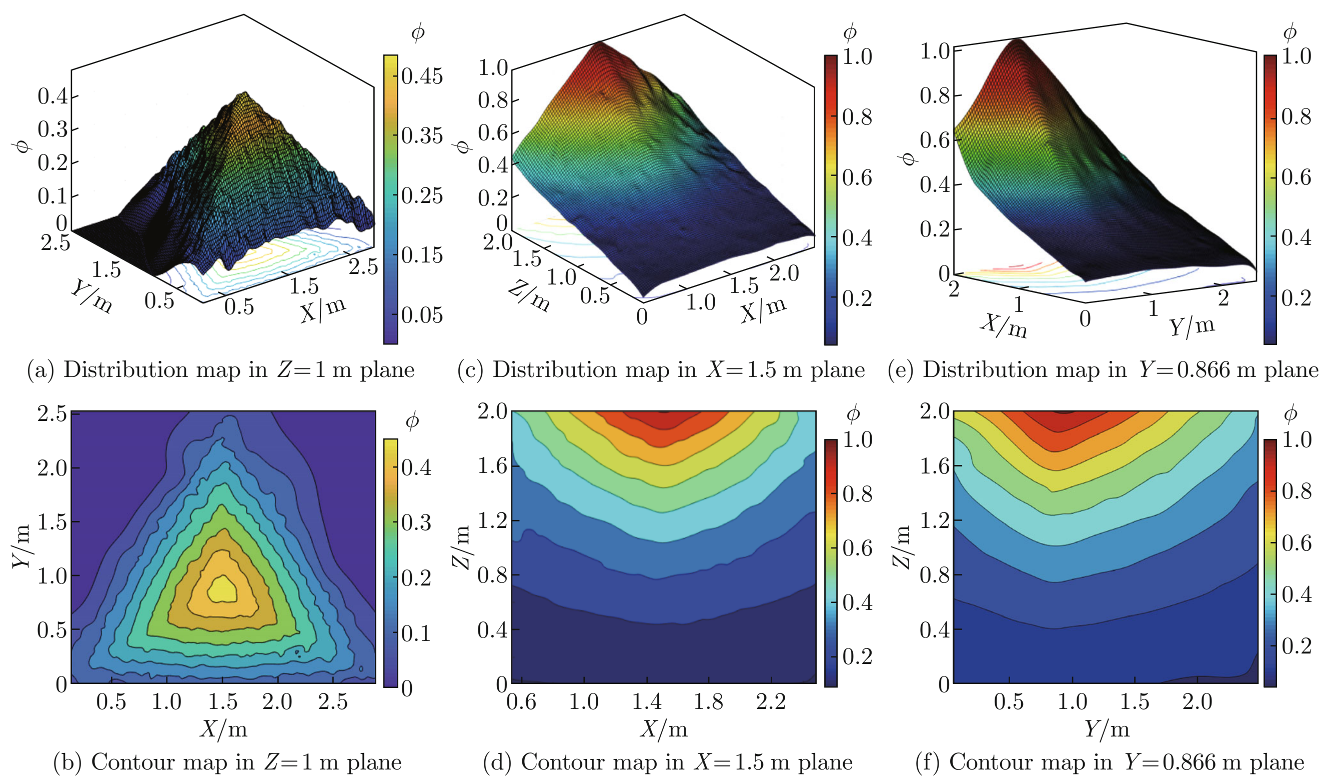

Fig. 3 Distribution map and contour map of the stability ($k_1 = 0.3$, $k_2 = 0.7$)

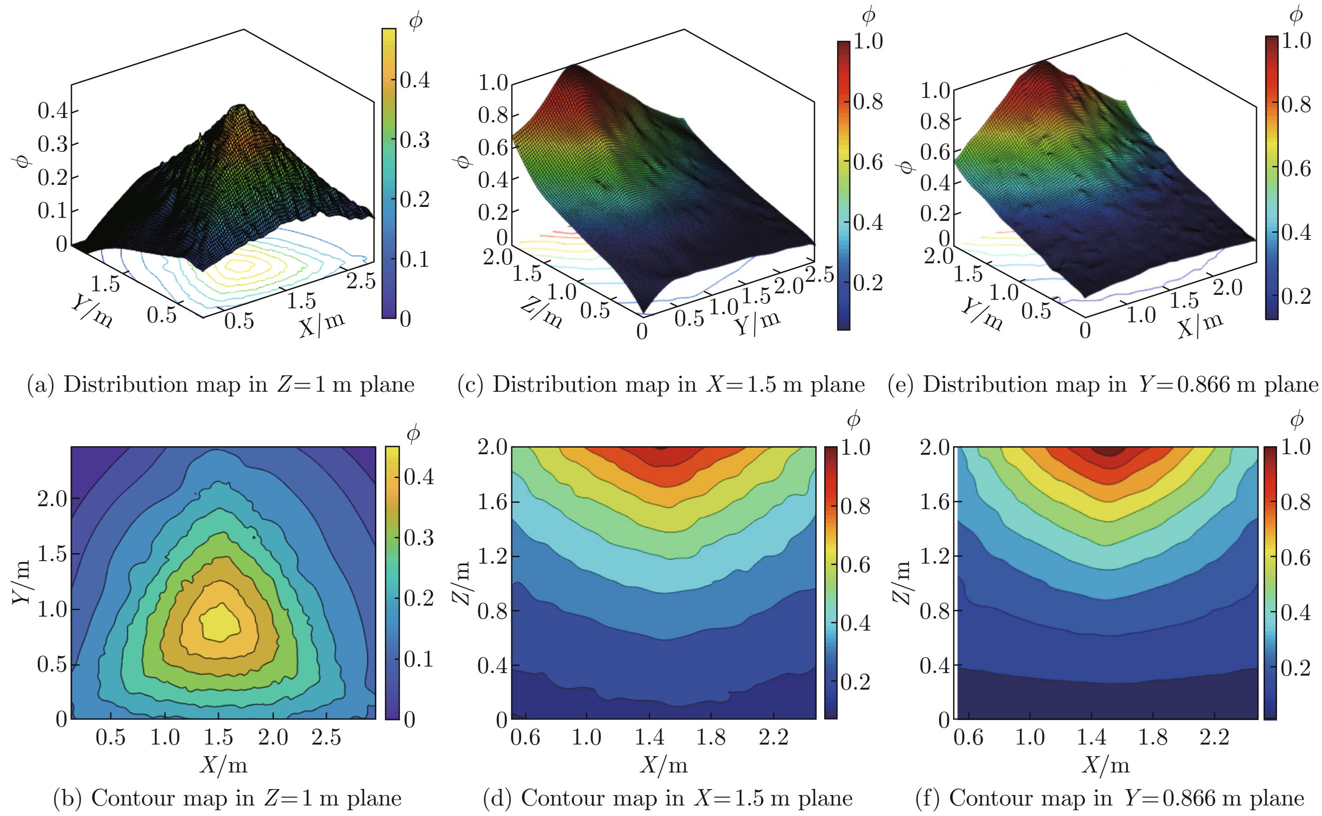

(a) Distribution map in $Z=1$ m plane (c) Distribution map in $X=1.5$ m plane (e) Distribution map in $Y=0.866$ m plane

(b) Contour map in $Z=1$ m plane (d) Contour map in $X=1.5$ m plane (f) Contour map in $Y=0.866$ m plane

Fig. 4 Distribution map and contour map of the stability ($k_1 = 0.5$, $k_2 = 0.5$)

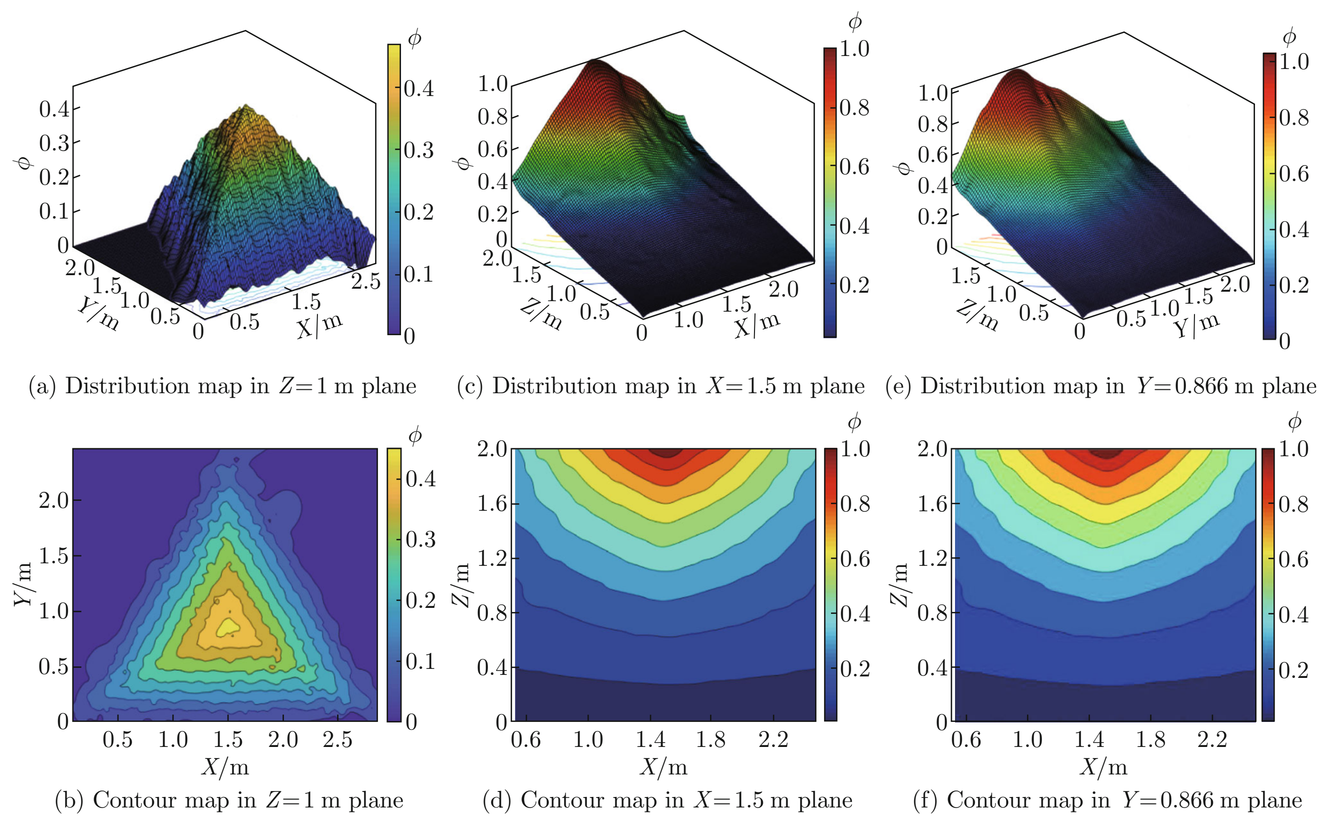

(a) Distribution map in $Z=1$ m plane (c) Distribution map in $X=1.5$ m plane (e) Distribution map in $Y=0.866$ m plane

(b) Contour map in $Z=1$ m plane (d) Contour map in $X=1.5$ m plane (f) Contour map in $Y=0.866$ m plane

Fig. 5 Distribution map and contour map of the stability ($k_1 = 0.7$, $k_2 = 0.3$)

singular value of the stiffness matrix, the boundary distortion and uneven contour distribution of the contour maps are improved. However, as the weighting coefficient of the minimum tension increases, the three edges of the triangle gradually become circular arcs. For $k_1 = 0.7$ and $k_2 = 0.3$, the triangular shape of the contour map does not deform, which retains the advantage of a single stability index. The weighting coefficient of the minimum tension should not be increased, otherwise the minimum tension index will have too much influence on the stability and lose its significance for a comprehensive evaluation.

Depending on the structure of the towing system, the workspace of the load is always in the triprism space formed by the endpoints of the three robots and their projected points in the horizontal plane. Points with stability over 0.4 are set as stability points. Therefore, the proportion of stability points to static workspace points in the three stages of towing is shown in Table 3 for different combinations of the weighting coefficients. It can be seen that the system has fewer stability points in both the second and third stages, indicating that the stability of the load is too low. By comparison, it is found that with the same weighting coefficient, the first stage is the largest, the second stage is the second largest, and the third stage is the smallest, indicating that the stability of the load gradually decreases during the towing process. Under the same towing stage, the load has the highest stability at $k_1 = 0.7$ and $k_2 = 0.3$. Therefore, the weighting coefficient of the minimum tension is chosen to be 0.7, and the weighting coefficient of the minimum singular value is chosen to be 0.3. In this way, it is relatively reasonable to comprehensively analyze the load stability of the floating multi-robot coordinated towing system.

Table 3 Proportion of stability points to workspace points

Stage	ϕ/%		
	$k_1 = 0.3$, $k_2 = 0.7$	$k_1 = 0.5$, $k_2 = 0.5$	$k_1 = 0.7$, $k_2 = 0.3$
First	75.3	78.6	81.8
Second	47.5	56.9	63.1
Third	36.7	40.2	45.3

By analyzing the load stability at different towing stages, not only the appropriate driving mode, but also the optimal weighting coefficient can be selected. In the meantime, the stability analysis of the load can provide guidance for the subsequent planning of movement trajectories with high stability.

5 Conclusion

The multi-robot coordinated towing system has become an important tool for towing in factories, railways, and ports, and has broad research prospects. In this paper, the configuration, dynamics, and load stability of the floating multi-robot coordinated towing system are studied, and the main conclusions are as follows:

(1) According to the motion characteristics of the floating multi-robot coordinated towing system, the method of judging the load stability is obtained by weighting the minimum tension of the ropes and the minimum singular value of the stiffness matrix.

(2) The different weighting coefficients are selected to analyze the stability of the load, separately, and a relatively reasonable weighting coefficient is obtained.

(3) The distribution of load stability in the workspace is obtained by simulation, which provides a basis for subsequent trajectory planning and anti-swing control.

Due to the complex working conditions of the floating multi-robot coordinated towing system, there are many factors that affect the load stability. As research deepens, more methods must be used to analyze the load stability of the towing system at later stages. In addition, the load stability is the subject of the present paper, and the stability of the whole towing system is not considered.

References

[1] SU C, YE J N, LI W, et al. Analysis of dynamic workspace for under-constrained coordinate suspending system with multi-robots [J]. *Journal of Shanghai Jiao Tong University*, 2019, **53**(2): 225-231 (in Chinese).

[2] SU C, ZHANG S H, LI W, et al. Research on tension optimization of under-constrained collaborative towing system with multi-helicopters in inverse dynamics [J]. *UPB Scientific Bulletin, Series D: Mechanical Engineering*, 2020, **82**(1): 79-92.

[3] ZHAO Z G, TENG F J, SHI G T, et al. Analysis and calculation of feasible region of multi-robot combined lifting system [J]. *Journal of Shanghai Jiao Tong University*, 2015, **49**(8): 1174-1180 (in Chinese).

[4] ZHAO Z G, LÜ T S, WANG G. Modeling of dynamic characteristic of small-scale robot helicopter system via takagi-sugeno fuzzy identification [J]. *Journal of Shanghai Jiao Tong University*, 2008, **42**(5): 856-860 (in Chinese).

[5] JIANG Q M, KUMAR V. Determination and stability analysis of equilibrium configurations of objects suspended from multiple aerial robots [J]. *Journal of Mechanisms and Robotics*, 2012, **4**(2): 1.

[6] JIANG Q M, KUMAR V. The inverse kinematics of cooperative transport with multiple aerial robots [J]. *IEEE Transactions on Robotics*, 2013, **29**(1): 136-145.

[7] HOROUB M, HAWWA M. Influence of cables layout on the dynamic workspace of a six-DOF parallel marine manipulator [J]. *Mechanism and Machine Theory*, 2018, **129**: 191-201.

[8] CHANDRASEKARAN S, JAIN A K. Triangular Configuration Tension Leg Platform behaviour under random sea wave loads [J]. *Ocean Engineering*, 2002, **29**(15): 1895-1928.

[9] MAO Y F, ZHU K Q, JING B, et al. Dynamic response analysis of two boat floating crane system in irregular waves [J]. *Journal of Waterway and Harbor*, 2017, **38**(1): 31-37 (in Chinese).

[10] MICHAEL N, FINK J, KUMAR V. Cooperative manipulation and transportation with aerial robots [J]. *Autonomous Robots*, 2011, **30**(1): 73-86.

[11] BOSSCHER P M. Disturbance robustness measures and wrench-feasible workspace generation techniques for rope-driven robots [D]. Atlanta: Georgia Institute of Technology, 2004.

[12] BEHZADIPOUR S, KHAJEPOUR A. Stiffness of cable-based parallel manipulators with application to stability analysis [J]. *Journal of Mechanical Design*, 2006, **128**(1): 303-310.

[13] CARRICATO M, MERLET J P. Stability analysis of underconstrained cable-driven parallel robots [J]. *IEEE Transactions on Robotics*, 2013, **29**(1): 288-296.

[14] LIU P. On the mechanics and stability for the cable-driven parallel manipulators [D]. Xi'an: Xidian University, 2014 (in Chinese).

[15] LIU P, QIUY Y. Approach with a hybrid force-position property to assessing the stability for camera robots [J]. *Journal of Xidian University* (*Natural Science*), 2016, **43**(1): 87-93 (in Chinese).

[16] WANG Y L. Modeling and stability analysis for cable-typing close-coupling multi-robots towing system [D]. Lanzhou: Lanzhou Jiaotong University, 2017 (in Chinese).

[17] ZHAO Z G, WANG Y L, LI J S, et al. Appraise of dynamical stability of multi-robots cooperatively lifting system based on hybrid force-position-pose approach [J]. *Journal of Harbin Engineering University*, 2018, **39**(1): 148-155 (in Chinese).

[18] SU C, LI J H, MA Y, et al. Motion analysis of an under-constrained multi-robots collaborative towing system based on stiffness [J]. *UPB Scientific Bulletin, Series D: Mechanical Engineering*, 2019, **81**(4): 5-16.

[19] LI H, ZHU W B. Static stiffness analysis of flexible-cable-driven parallel mechanism [J]. *Journal of Mechanical Engineering*, 2010, **46**(3): 8-16 (in Chinese).

[20] TIAN S X. Diagonally dominant matrix [M]. Beijing: Posts and Telecommunications Press, 2007 (in Chinese).